

Long-term Microscopic Traffic Simulation with History-Masked Multi-agent Imitation Learning

Ke Guo^{1,2}, Wei Jing², Lingping Gao², Weiwei Liu², and Weizi Li³, Jia Pan¹

¹ The University of Hong Kong, {kguo, jpan}@cs.hku.hk

² Alibaba Group {21wjing, gaolingping.glp}@gmail.com,
11932061@zju.edu.cn

³ University of Memphis wli@memphis.edu

Abstract: A realistic long-term microscopic traffic simulator is necessary for understanding how microscopic changes affect traffic patterns at a larger scale. Traditional simulators that model human driving behavior with heuristic rules often fail to achieve accurate simulations due to real-world traffic complexity. To overcome this challenge, researchers have turned to neural networks, which are trained through imitation learning from human driver demonstrations. However, existing learning-based microscopic simulators often fail to generate stable long-term simulations due to the *covariate shift* issue. To address this, we propose a history-masked multi-agent imitation learning method that removes all vehicles’ historical trajectory information and applies perturbation to their current positions during learning. We apply our approach specifically to the urban traffic simulation problem and evaluate it on the real-world large-scale pNEUMA dataset, achieving better short-term microscopic and long-term macroscopic similarity to real-world data than state-of-the-art baselines.

Keywords: Traffic Simulation, Multi-Agent Imitation Learning

1 Introduction

Microscopic traffic simulators are powerful tools for transportation engineers and planners to analyze and predict the impact of microscopic adjustments on traffic patterns without disrupting real-world traffic. For example, it can help analyze how changing road shape like replacing an intersection with a roundabout affects traffic patterns [1], and develop traffic-aware autonomous driving policies that enhance overall traffic efficiency [2, 3]. However, creating a realistic simulator that can simultaneously replicate the microscopic response of human drivers to traffic conditions and the resulting long-term macroscopic statistics is a challenging task.

In recent years, there have been significant efforts to develop realistic traffic simulators that accurately model human driving behavior. Traditional traffic simulators, such as SUMO [4], AIMSUN [5], and MITSIM [6], typically rely on heuristic car-following models like the Intelligent Driver Model (IDM) [7]. However, despite careful calibration of parameters, these simplified, rule-based models often fail to deliver accurate simulations [8] due to the complexity of real-world traffic environments. Factors such as road structure, neighboring vehicles, and even driver psychology can influence human driver decision-making, making it challenging to achieve accurate simulations.

To improve the capabilities of traffic simulators, researchers have turned to neural networks as a driving model. These models are trained through imitation learning (IL) from human driver demonstrations. Most studies [9, 10] employ behavior cloning (BC) [11] to learn the driving policy in a supervised fashion by minimizing the difference between the model output and the human driver’s action in the training state distribution. However, the BC method suffers from the *covariate*

shift issue [12], where the state induced by the learner’s policy deviates cumulatively from the expert’s distribution.

To address this issue, recent works [13] propose using generative adversarial imitation learning (GAIL) [14]. GAIL learns a reward function by a discriminator neural network and trains the policy network to maximize the reward through online reinforcement learning. This allows agents to learn to recover from out-of-distribution states. However, directly applying GAIL to the traffic simulation problem, which is a multi-agent imitation learning task, is problematic because the environment changes during the policy learning process, leading to highly biased estimated gradients. To mitigate this instability, the parameter-sharing generative adversarial imitation learning (PS-GAIL) [13] makes all agents share the policy and critic parameter and gradually increases the agent numbers. However, even in a simple highway environment, there are many undesirable off-road driving cases [15], which limit the effectiveness of PS-GAIL.

Although existing learning-based microscopic simulators have shown success in short-term simulation applications, such as autonomous driving tests [10, 16], they often fail to generate stable long-term traffic simulations. Hence, we propose a history-masked multi-agent imitation learning (HMMIL) method that can remove all agents’ historical trajectory information and apply a perturbation to their current positions during learning. Our method is inspired by context-conditioned imitation learning (CCIL) [17], a single-agent offline imitation learning method for autonomous driving.

CCIL solves the *covariate shift* issue in BC for autonomous driving by removing the ego vehicle’s historical trajectories and adding perturbations to its current position because the ego state is highly susceptible to policy errors, while human drivers in the context are assumed to be robust to the ego vehicle’s policy error. However, directly applying CCIL to the multi-agent imitation learning problem by making all agents share the same policy works poorly because other vehicles’ behaviors are also directly determined by the learned policy, unlike in the autonomous driving task. This leads to an additional *covariate shift* in the context. To overcome this problem, our method removes the histories of all vehicles and adds perturbation to all vehicles instead of only the ego vehicle in CCIL.

The main contributions of our paper are:

- We propose a new history-masked multi-agent imitation learning (HMMIL) method that can address the *covariate shift* issue in multi-agent imitation learning.
- We apply our approach specifically to urban traffic simulation. To the best of our knowledge, this is the first imitation learning-based traffic simulator that can reproduce long-term (more than 10 minutes) microscopic urban traffic.
- We evaluate our method on a real-world large-scale dataset, named pNEUMA [18], achieving better short-term microscopic and long-term macroscopic similarity to real-world data than state-of-the-art baselines. The videos and code for our method can be found at <https://sites.google.com/view/hmmil>.

2 Related Work

While macroscopic traffic simulators in [19, 20, 21] can efficiently reproduce long-term macroscopic statistics, they are incapable of analyzing the effects of microscopic changes. Therefore, we focus on microscopic traffic simulators that can capture detailed interactions between vehicles and accurately replicate human driving behavior. These simulators can be classified into rule-based and learning-based simulators based on their driving models.

2.1 Rule-based Simulator

Rule-based models like the IDM [7] and Krauss model [22] have been widely applied in popular traffic simulators such as SUMO [4], AIMSUN [5], and MITSIM [6]. These models describe individual vehicle behavior based on a car-following model that predicts the longitudinal

acceleration of a vehicle based on its relative speed and distance to its front vehicle. Although there are some parameter calibration methods [23, 24] using real data, these models are oversimplified in their assumptions of interactions between traffic participants and are therefore limited in their accuracy.

2.2 Learning-based Simulator

To improve the modeling capacity and similarity to human behavior, recent studies have attempted to learn a neural driving model by imitation from human driving demonstrations. These methods can be generally classified into BC-based and GAIL-based methods.

BC-based methods, such as TrafficSim [10] and SimNet [16], usually first learn a prediction model and then modify the predicted trajectories to avoid collisions and traffic rule violations during simulation. However, these BC-based methods cannot achieve long-term simulation due to the *covariate shift* problem caused by the discrepancy between the distribution of the training data and the learned policy’s state distribution. In contrast, our method is learned offline like BC, but we address the *covariate shift* problem by ignoring historical trajectories and blurring current positions, thus achieving long-term stable simulation. To improve performance, we also modify the predicted trajectory by projecting it onto the road and making it smooth from the current state during simulation, but skip the computationally costly collision removal operation because we mainly focus on the long-term macroscopic influence.

GAIL-based methods [13, 15, 25] learn the hidden reward function of human driving behavior and obtain the driving policy by maximizing the learned reward. While GAIL can theoretically address the *covariate shift* of BC in a single-agent context by online interaction, its performance deteriorates when applied to the multi-agent imitation learning domain due to the dynamic environment, leading to a tricky training process. To address this issue, PS-GAIL [13] requires two-stage learning and gradually adds vehicles to the environment. However, PS-GAIL still exhibits a significant number of undesirable traffic phenomena, such as off-road driving, collisions, and hard braking. Based on PS-GAIL, the reward-augmented imitation learning (RAIL) method [15, 25] penalizes undesirable phenomena by adding a hand-crafted reward, but maximizing the new reward does not guarantee the recovery of human-like trajectories. Despite many improvements on the original GAIL, these GAIL-based methods usually fail to produce stable long-term traffic flow, as demonstrated in our experiments. In contrast, our method is an offline supervised learning method, leading to faster, simpler, and more stable learning of human driving policy.

3 Method

In Fig. 1, we present an overview of our method. Our method predicts vehicles’ future trajectory distribution using a graph neural network, where their history information is overlooked during learning. During simulation, we yield a smooth action for each vehicle based on sampled positions from the predicted distribution and its current state.

3.1 Traffic Graph Representation

In the traffic system, a human driver makes decisions mainly depending on its neighboring context including other vehicles and road network. Therefore, we can model the system with a graph by connecting neighboring elements.

Note: To save computational cost, we only create agent nodes and assign road information to them. Each agent node has input features including its type, destination position, nearest routing points with corresponding road width, and the traffic light status of its closest road. The agent’s history is not taken into account to avoid the *covariate shift* issue. Because each agent’s routing information contains partial road network information, each agent can still obtain its neighboring road network information by exchanging information with neighboring agents. To improve the model’s generalizability, we transform each node feature to its individual coordinate system. We

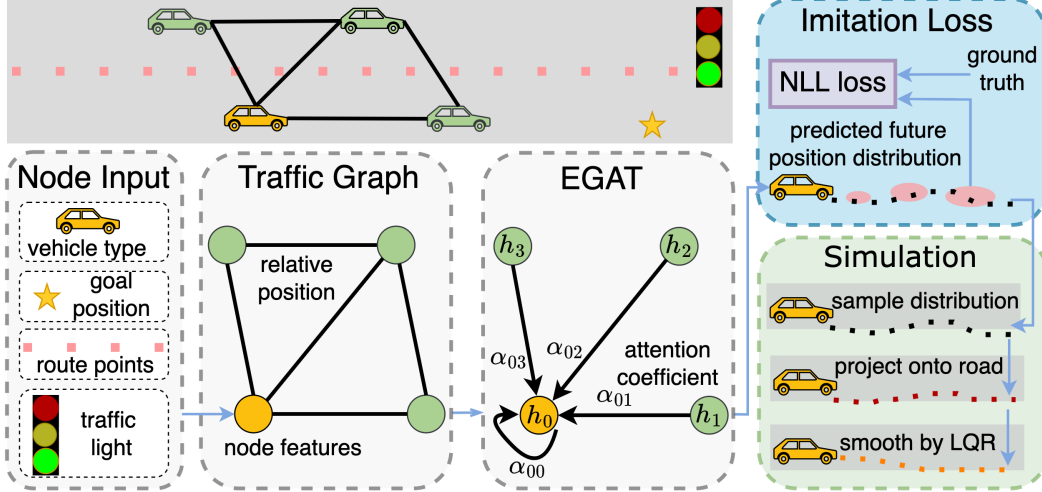


Figure 1: Overview of our approach.

use the ego-perturbed goal-oriented coordinate system described in CCIL [17], where the origin is the agent’s current position plus a zero-mean Gaussian perturbation, and the x -axis direction points towards its goal position.

Edge: When transforming each agent’s state coordinates from the global coordinate system to their individual coordinate system, information about the relative positions among agents is lost. However, a traffic model needs to consider the relative configuration of agents to understand how they interact with each other. To preserve these relationships, we introduce directed edges among neighboring agents. The edge feature is the relative position of the destination node in the source node’s coordinate system. In practice, we connect an agent with its nearest 8 neighbors located within a neighborhood distance of 30 meters.

3.2 Edge-enhanced Graph Attention Network

To predict the future position distribution of all agents, we utilize an edge-enhanced graph attention network (EGAT) [26, 27]. EGAT is a variant of graph attention networks (GAT) [28] that can efficiently model interactions by aggregating neighboring node information using an attention mechanism. However, traditional GAT can only handle node features, while our traffic graph’s edges contain relative position information. EGAT overcomes this challenge by concatenating edge features with connected node features to perform aggregation. In each EGAT layer, the node’s next state is calculated as follows:

$$\mathbf{h}_i^l = \sigma \left(\sum_{j \in \mathcal{N}_i} \alpha_{ij}^l \mathbf{W}^l \left[\mathbf{h}_i^{(l-1)} \| \mathbf{e}_{ij} \| \mathbf{h}_j^{(l-1)} \right] \right), \quad (1)$$

where \mathbf{h}_i^l is the feature of node i in the l th layer, \mathbf{e}_{ij} is the position of node j relative to node i , \mathbf{W}^l is the learnable weight matrix, \mathcal{N}_i is the set of the first-order neighbors of node i (including the node itself), and σ is a non-linear activation function. The node features at the first layer are obtained by embedding the node input features with multi-layer perceptions (MLPs). The attention coefficient α_{ij}^l indicates the importance of node j to node i , considering both node and edge features, and is computed as:

$$\alpha_{ij}^l = \text{softmax}_j \left(\sigma \left((\mathbf{a}^l)^T \left[\mathbf{h}_i^{(l-1)} \| \mathbf{e}_{ij} \| \mathbf{h}_j^{(l-1)} \right] \right) \right), \quad (2)$$

where \mathbf{a}^l is a learnable weight vector, and normalization is performed on the weights across all neighbors of node i using a softmax function.

3.3 Imitation Loss

After passing through multiple EGAT layers, the hidden state of each node m is fed into a fully connected layer to predict its future position distribution over T time steps, denoted as $p(\hat{\mathbf{p}}_1^m, \hat{\mathbf{p}}_2^m, \dots, \hat{\mathbf{p}}_T^m)$, which is assumed to be a product of multi-variable Gaussian distributions:

$$p(\hat{\mathbf{p}}_1^m, \hat{\mathbf{p}}_2^m, \dots, \hat{\mathbf{p}}_T^m) = \prod_{t=1}^T \mathcal{N}(\hat{\boldsymbol{\mu}}_t^m, \hat{\boldsymbol{\Sigma}}_t^m), \quad (3)$$

where $\hat{\boldsymbol{\mu}}_t^m$ and $\hat{\boldsymbol{\Sigma}}_t^m$ represent the mean and covariance matrix of the predicted position $\hat{\mathbf{p}}_t^m$ at future time step t , respectively. For simplicity, we assume that there is no correlation between the position distributions at different future time steps. To learn the graph neural network, we minimize the negative log-likelihood (NLL) loss of all agents' ground-truth future trajectories:

$$\mathcal{L} = - \sum_{m=1}^M \sum_{t=1}^T \log(\mathcal{N}(\mathbf{p}_t^m - \hat{\boldsymbol{\mu}}_t^m, \hat{\boldsymbol{\Sigma}}_t^m)), \quad (4)$$

where \mathbf{p}_t^m denotes the ground truth position of agent m at future time step t , and M is the total number of agents in the traffic graph.

3.4 Simulation Process

During the simulation process, we use the predicted future position distribution to calculate the next position of each agent. Firstly, we sample from the distribution, and then project each sampled position onto the nearest point on the road. Finally, we smooth the projected trajectory with a linear-quadratic regulator (LQR) [29] to ensure the feasibility and smoothness of the simulated trajectory. The LQR algorithm can efficiently minimize the total commutative quadratic cost of a linear dynamic system. We consider a finite-horizon, discrete-time linear system with dynamics described by:

$$\begin{bmatrix} \tilde{\mathbf{p}}_{t+1}^m \\ \tilde{\mathbf{v}}_{t+1}^m \end{bmatrix} = \begin{bmatrix} \mathbf{I} & \mathbf{D} \\ 0 & \mathbf{I} \end{bmatrix} \begin{bmatrix} \tilde{\mathbf{p}}_t^m \\ \tilde{\mathbf{v}}_t^m \end{bmatrix} + \begin{bmatrix} \mathbf{D}^2 \\ \mathbf{D} \end{bmatrix} \tilde{\mathbf{a}}_t^m, \quad (5)$$

where \mathbf{D} is a diagonal matrix with the interval of each time step as diagonal entries, and $\tilde{\mathbf{p}}_t^m$, $\tilde{\mathbf{v}}_t^m$, $\tilde{\mathbf{a}}_t^m$ represent the LQR-planned position, velocity, and acceleration, respectively. The system is subject to a quadratic cost function:

$$\mathcal{J} = \sum_{m=1}^M \sum_{t=1}^T \|\tilde{\mathbf{p}}_t^m - \bar{\mathbf{p}}_t^m\|^2 + \eta_a \|\tilde{\mathbf{a}}_t^m\|^2, \quad (6)$$

where the projected predicted position $\tilde{\mathbf{p}}_t^m$ is considered as the target pose, and the hyper-parameter η_a is used to penalize high acceleration. After the LQR optimization, each agent is updated to the first position of the planned trajectory.

4 Experiment

4.1 Dataset

We use a real-world dataset called **pNEUMA** [18] to construct a realistic urban traffic simulator. This dataset contains over half a million trajectories of various types of vehicles, collected by 10 drones in Athens over 4 days. The drones recorded traffic streams in a large area with over 100 km of lanes in the road network and around 100 busy intersections (signalized or not). However, since the dataset did not provide traffic light states, we designed an algorithm to estimate this information from the recorded trajectory data, which is described in the appendix.

The recordings were done at 5 periods during each day, spanning about 15 minutes each, with a time interval of collected data being 0.04 seconds. To enhance computation efficiency, we use a time step of 0.4 seconds. We split the dataset into a training set (recordings from the first 3 days) and

a validation/test set (recordings from the last day). We do not use other popular datasets for traffic simulation, such as NGSIM [30] or HighD [31], because they only contain simple highway scenarios without traffic lights, making it challenging to develop a generalizable urban traffic simulator.

4.2 Metrics

We evaluate the realism of our simulator by measuring the similarity between the simulation result and real data. During evaluation, we assume that each vehicle enters the simulator at its first recorded time and position, and is then controlled by our simulator to complete its recorded route. When an agent reaches its final recorded position, it is removed from the simulator.

Firstly, we follow prior works [13, 15] and conduct a **short-term microscopic** evaluation by simulating for 20 seconds from a random time step in the test dataset. We measure the similarity between the simulated and real data using **position and velocity RMSE** metrics, which are calculated by:

$$\text{RMSE} = \frac{1}{T_s} \sum_{t=1}^{T_s} \sqrt{\frac{1}{M} \sum_{m=1}^M \|s_t^m - \hat{s}_t^m\|^2}, \quad (7)$$

where s_t^m and \hat{s}_t^m were the real and simulated value of the position or velocity of the agent m at time step t , respectively. T_s was the total simulated time steps, and M was the total simulated agent number. We also calculate the **off-road rate**, which measures the average proportion of vehicles that deviate more than 1.5 meters from the road over all time steps. We do not measure the common collision rate metric because we focus on the long-term influence of the traffic model and the dataset does not provide accurate vehicle size and heading information.

In addition, we also evaluate our model’s **long-term macroscopic** accuracy on five periods in the test dataset for 800 seconds from its initial recording time. To measure the long-term performance, we use two common macroscopic metrics for traffic flow data [19, 20, 21], namely **road density and speed RMSE**, in addition to the **off-road rate**. The density of a road at a time step is calculated by dividing the number of vehicles on the road by its total lane length, assuming that all lanes have the same width. Meanwhile, the road speed is computed as the mean speed of all vehicles on the road. To quantify the similarity between the simulated and ground truth values, we still use RMSE in Eq. (7), where the variable M becomes the total number of roads in the recorded area.

4.3 Performance

We conduct a comparative analysis of our method against several baselines, including one rule-based method (SUMO), two GAIL-based methods (PS-GAIL and RAIL), and two BC-based methods (BC and PS-CCIL):

SUMO [4]: we use the IDM model [7] as the car-following model and mobil [32] as the lane-changing model. We tune the IDM’s parameters by minimizing the MSE between the IDM calculated acceleration and real acceleration using an Adam optimizer [33].

PS-GAIL [13]: we learn our model based on GAIL and let all vehicles share the same policy parameter and critic parameter with the PPO [34] as the reinforcement learning algorithm.

RAIL [15]: we use the same learning process as **PS-GAIL** but with an additional off-road penalty.

BC [11]: we learn our model structure directly by BC without removing the context history or perturbing the historical trajectory.

Parameter-Sharing CCIL (PS-CCIL): we directly extend the CCIL method [17] by making all vehicle sharing the same policy parameter without removing the context history.

We train and evaluate each model three times to obtain the mean and standard deviation (std) of various metrics. We evaluate both short-term and long-term performance, as shown in Tables 1 and 2, respectively. Our method achieves better results than all baselines in terms of position and velocity RMSE, road density and speed RMSE, with minor off-road rate.

Table 1: Comparison with baselines on microscopic metrics for 20 seconds

Model	Position RMSE(m)	Velocity RMSE(m/s)	Off-road(%)
SUMO [4]	41.25	7.00	0
PS-GAIL [13]	61.65±2.56	6.67±0.32	1.72±0.13
RAIL [15]	55.78±2.47	5.93±0.19	0.59±0.04
BC [11]	39.95±1.53	6.60±0.23	31.80±2.12
PS-CCIL	18.45±0.51	2.80±0.05	0.45±0.02
HMMIL (ours)	18.10±0.65	2.72±0.08	0.28±0.01

Table 2: Comparison with baselines and ablated models on macroscopic metrics for 800 seconds

Model	Road Density RMSE(veh/km)	Road Speed RMSE(m/s)	Off-road(%)
SUMO [4]	52.70	5.52	0
PS-GAIL [13]	90.34±5.67	5.63±0.20	37.62±3.24
RAIL [15]	170.34±8.45	5.38±0.24	4.28±0.10
BC [11]	44.84±1.18	4.91±0.12	70.42±5.23
PS-CCIL	62.11±0.43	2.88±0.08	0.53±0.03
HMMIL (ours)	38.71±0.18	2.55 ±0.13	0.31±0.02
w History	57.17±0.42	4.77±0.29	0.59±0.04
w/o Perturb	59.58±0.45	2.75±0.13	0.78±0.03
w/o Project	38.06±0.13	2.58±0.14	1.05±0.05
w/o LQR	38.87±0.21	4.07±0.17	0.28±0.02

4.4 Ablation Study

To expose the significance of different components of our model on long-term performance, we conducted several ablation experiments, and their results are presented in Tab. 2:

History removal: To study the importance of removing explicit historical information from the network input, we reintroduce the historical information by concatenating each vehicle’s past positions with current node inputs. We observe a drop in performance due to the *covariate shift* issue.

Position perturbation: We remove the position perturbation in each agent’s individual coordinate system to analyze its impact. It demonstrates that the perturbation can improve long-term performance by reducing the influence of the current position.

On-road projection: We ablate the on-road projection module to demonstrate its importance in reducing off-road rate. The results show that it leads to a small decrease in road density but significantly increases the off-road rate.

LQR: To demonstrate the effectiveness of the LQR module, we remove it from our model. It demonstrates that while the LQR leads to higher road density RMSE and off-road rate due to more constrained movement, removing it significantly increases the road speed RMSE.

4.5 Qualitative Result

In Fig. 2, we present the mean road density and speed for real-world data, SUMO simulation, and our proposed method over all time steps. The figure shows that our proposed method accurately reproduces long-term macroscopic traffic patterns, outperforming the SUMO simulator.

In Fig. 3, we present the mean road density and speed changes in our simulator after modifying several roads’ shapes. We can see that a local modification can have a global influence.

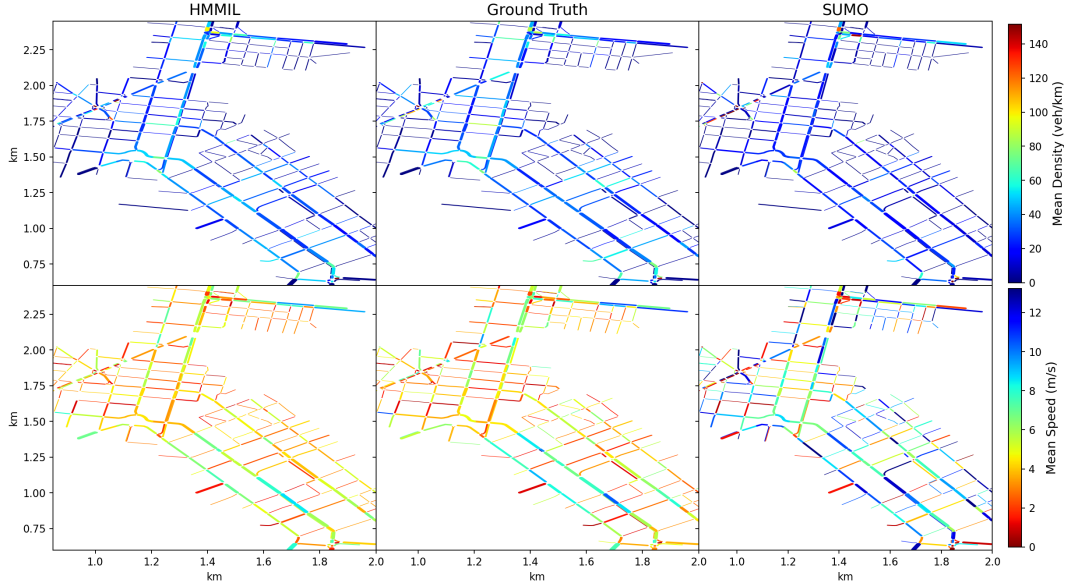


Figure 2: Mean density and speed on each road over all time steps in the long-term evaluation.

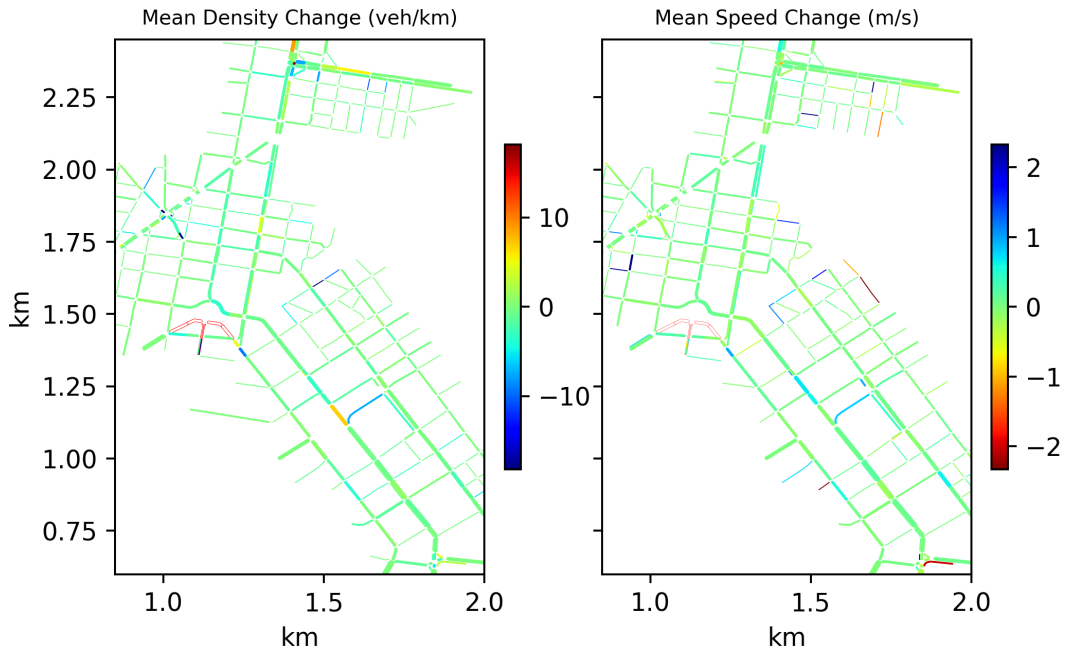


Figure 3: Mean density and speed changes after modifying road network.

5 Limitation

There are two main limitations of our simulator. Firstly, even though removing all history information is a simple way to create a long-term simulation, some history information may be important for microscopic decision-making. To create a more realistic human driving model with history information input, a new method that can address the *covariate shift* problem in the history and context needs to be developed, as existing GAIL-based multi-agent imitation learning methods perform poorly in practice. Secondly, although the **pNEUMA** dataset records a large area with thousands of vehicles, it does not provide accurate vehicle shape, heading, high-definition map, and traffic light information. Therefore, our learned model’s microscopic performance is limited by the data accuracy. Future work could focus on improving the data accuracy or exploring alternative data sources to address the limitation.

6 Conclusion

In conclusion, we propose a history-masked multi-agent imitation learning method for realistic long-term microscopic traffic simulation. Our method addresses the *covariate shift* issue in multi-agent imitation learning, allowing us to generate stable long-term traffic simulations that are essential for transportation planning and developing more traffic-aware autonomous driving policies. We apply our approach specifically to the urban traffic simulation problem and achieve better short-term microscopic and long-term macroscopic similarity to real-world data than state-of-the-art baselines.

References

- [1] J. Bared and P. Edara. Simulated capacity of roundabouts and impact of roundabout within a progressed signalized road. *Transportation research circular*, 2005, 2005.
- [2] L. Y. Zheng, S. Son, and M. C. Lin. Traffic-aware autonomous driving with differentiable traffic simulation. In *International Conference on Robotics and Automation (ICRA)*, 2023.
- [3] D. Wang, W. Li, L. Zhu, and J. Pan. Learning to control and coordinate hybrid traffic through robot vehicles at complex and unsignalized intersections. *ArXiv*, abs/2301.05294, 2023.
- [4] D. Krajzewicz, J. Erdmann, M. Behrisch, and L. Bieker. Recent development and applications of SUMO-Simulation of Urban MObility. *International journal on advances in systems and measurements*, 5(3&4), 2012.
- [5] J. Barceló and J. Casas. Dynamic network simulation with aimsun. *Simulation approaches in transportation analysis: Recent advances and challenges*, pages 57–98, 2005.
- [6] Q. Yang and H. N. Koutsopoulos. A microscopic traffic simulator for evaluation of dynamic traffic management systems. *Transportation Research Part C: Emerging Technologies*, 4(3): 113–129, 1996.
- [7] M. Treiber, A. Hennecke, and D. Helbing. Congested traffic states in empirical observations and microscopic simulations. *Physical review E*, 62(2):1805, 2000.
- [8] S. Feng, X. Yan, H. Sun, Y. Feng, and H. X. Liu. Intelligent driving intelligence test for autonomous vehicles with naturalistic and adversarial environment. *Nature Communications*, 12, 2021.
- [9] J. Morton, T. A. Wheeler, and M. J. Kochenderfer. Analysis of recurrent neural networks for probabilistic modeling of driver behavior. *IEEE Transactions on Intelligent Transportation Systems (TITS)*, 18(5):1289–1298, 2016.
- [10] S. Suo, S. Regalado, S. Casas, and R. Urtasun. TrafficSim: Learning to simulate realistic multi-agent behaviors. In *IEEE/CVF Conference on Computer Vision and Pattern Recognition (CVPR)*, pages 10400–10409, 2021.
- [11] D. Michie, M. Bain, and J. Hayes-Michie. Cognitive models from subcognitive skills. *IEEE control engineering series*, 44:71–99, 1990.
- [12] S. Ross, G. Gordon, and D. Bagnell. A reduction of imitation learning and structured prediction to no-regret online learning. In *International Conference on Artificial Intelligence and Statistics (AISTATS)*, pages 627–635, 2011.
- [13] J. Song, H. Ren, D. Sadigh, and S. Ermon. Multi-agent generative adversarial imitation learning. *Advances in neural information processing systems*, 31, 2018.
- [14] J. Ho and S. Ermon. Generative adversarial imitation learning. *Advances in neural information processing systems*, 29, 2016.

- [15] R. P. Bhattacharyya, D. J. Phillips, C. Liu, J. K. Gupta, K. Driggs-Campbell, and M. J. Kochenderfer. Simulating emergent properties of human driving behavior using multi-agent reward augmented imitation learning. *International Conference on Robotics and Automation (ICRA)*, pages 789–795, 2019.
- [16] L. Bergamini, Y. Ye, O. Scheel, L. Chen, C. Hu, L. D. Pero, B. Osinski, H. Grimmer, and P. Ondruska. SimNet: Learning reactive self-driving simulations from real-world observations. *IEEE International Conference on Robotics and Automation (ICRA)*, pages 5119–5125, 2021.
- [17] K. Guo, W. Jing, J. Chen, and J. Pan. CCIL: Context-conditioned imitation learning for urban driving. In *Robotics: Science and Systems (RSS)*, 2023.
- [18] E. Barmponakis and N. Geroliminis. On the new era of urban traffic monitoring with massive drone data: The pNEUMA large-scale field experiment. *Transportation research part C: emerging technologies*, 111:50–71, 2020.
- [19] M. J. Lighthill and G. B. Whitham. On kinematic waves ii. a theory of traffic flow on long crowded roads. *Proceedings of the Royal Society of London. Series A. Mathematical and Physical Sciences*, 229(1178):317–345, 1955.
- [20] P. I. Richards. Shock waves on the highway. *Operations research*, 4(1):42–51, 1956.
- [21] J. Sewall, D. Wilkie, P. Merrell, and M. C. Lin. Continuum traffic simulation. In *Computer Graphics Forum*, number 2, pages 439–448, 2010.
- [22] S. Krauß. Microscopic modeling of traffic flow: Investigation of collision free vehicle dynamics, 1998.
- [23] A. Kesting and M. Treiber. Calibrating car-following models by using trajectory data: Methodological study. *Transportation Research Record*, 2088(1):148–156, 2008.
- [24] C. Osorio and V. Punzo. Efficient calibration of microscopic car-following models for large-scale stochastic network simulators. *Transportation Research Part B: Methodological*, 119: 156–173, 2019.
- [25] Y. Koeberle, S. Sabatini, D. V. Tsishkou, and C. Sabourin. Exploring the trade off between human driving imitation and safety for traffic simulation. *IEEE International Conference on Intelligent Transportation Systems (ITSC)*, pages 779–786, 2022.
- [26] F. Diehl, T. Brunner, M. T. Le, and A. Knoll. Graph neural networks for modelling traffic participant interaction. In *IEEE Intelligent Vehicles Symposium (IV)*, pages 695–701, 2019.
- [27] X. Mo, Z. Huang, Y. Xing, and C. Lv. Multi-agent trajectory prediction with heterogeneous edge-enhanced graph attention network. *IEEE Transactions on Intelligent Transportation Systems (TITS)*, 23:9554–9567, 2022.
- [28] P. Veličković, G. Cucurull, A. Casanova, A. Romero, P. Liò, and Y. Bengio. Graph attention networks. In *International Conference on Learning Representations (ICLR)*, 2018.
- [29] K. J. Åström and R. M. Murray. *Feedback systems: an introduction for scientists and engineers*. Princeton University Press, 2021.
- [30] J. Colyar and J. Halkias. Us highway 101 dataset. *Federal Highway Administration (FHWA), Tech. Rep.*, 2007.
- [31] R. Krajewski, J. Bock, L. Kloeker, and L. Eckstein. The highD dataset: A drone dataset of naturalistic vehicle trajectories on german highways for validation of highly automated driving systems. In *International Conference on Intelligent Transportation Systems (ITSC)*, pages 2118–2125, 2018.

- [32] A. Kesting, M. Treiber, and D. Helbing. General lane-changing model MOBIL for car-following models. *Transportation Research Record*, 1999(1):86–94, 2007.
- [33] D. Kingma and J. Ba. Adam: A method for stochastic optimization. *CoRR*, abs/1412.6980, 2014.
- [34] J. Schulman, F. Wolski, P. Dhariwal, A. Radford, and O. Klimov. Proximal policy optimization algorithms. *ArXiv*, abs/1707.06347, 2017.
- [35] W. Meert and M. Verbeke. Hmm with non-emitting states for map matching. In *European Conference on Data Analysis (ECDA), Germany*, 2018.

A Dataset Preparation

In the section, we introduce the data preparation process of pNEUMA dataset.

A.1 Trajectory Data

The trajectory data is downloaded from the official website (<https://open-traffic.epfl.ch>), specifically the data recorded by ALL Drones during all periods except for the first period (8.30-9.00 at 2018/10/24) due to a large position error caused by wind gusts.

A.2 Routing

To determine the route for each vehicle trajectory, we used the method proposed in [35]. However, this method generated many circular routes that are rarely observed in real data. To address this issue, we skipped the intermediate routing node points if they were far away from the actual trajectory, which helped reduce the number of unrealistic circular routes.

A.3 Road Network

The map information is downloaded from OpenStreetMap, and then we import it into SUMO to generate the road network. We only include highways for vehicles in the road network while excluding other road types, such as sidewalks and railways. However, we find that the map data is not always accurate, so we manually adjust the road shapes to reduce the number of off-road driving cases in the recorded trajectory data. Additionally, we modify the lane connection relations in junctions to alleviate traffic jams during SUMO simulations.

A.4 Traffic Light

Because the traffic light information is not provided by the dataset, we design an algorithm to estimate traffic light information from the recorded trajectory data.

Firstly, we filter all vehicle starting and stopping points near all signaled intersections from the trajectory data.

Secondly, we cluster these points based on their located edge, as we assume that all lanes on one edge are controlled by the same traffic light.

Thirdly, we obtain all time steps when each traffic light turns green by identifying its corresponding clustered points whose time gap to the previous point is larger than seven seconds. Similarly, we can obtain all time steps when it turns red.

Fourthly, based on all the time steps when the traffic light turns green, we need to calculate the traffic light’s first turning green time step, green time, and cycle length. We assume that all traffic lights in the same junction have the same cycle length, which can only be 45 or 90 seconds. To estimate the first green time and cycle length, we use a cost function, where a negative cost is given if the

filtered turning green time steps match the estimated turning green time step, and a positive cost is given if there is no filtered turning green time step matching the estimated turning green time step. By enumerating all first turning green time steps with an interval of 0.01 seconds, and cycle length of 45 or 90 seconds, we output the result with the minimal costs. Based on the other traffic light turning green time steps in the same junction, we can obtain its turning red time. If there is no other traffic light in the same junction, we need to estimate its turning red time as we do in the estimation of green time. Based on the turning red time and the turning green time, we can obtain the green time of each traffic light.

B Implementation details

B.1 Model Details

The hyper-parameters of our model architecture are listed in Tab. 3.

Table 3: Hyper-parameters

Hyper-parameter	Value
Future steps T	10
Route point number	50
MLP layer number	2
MLP hidden size	256
EGAT layer number L	5
EGAT hidden size	256
EGAT attention dropout	0.1
LQR acceleration weight η_α	1

B.2 Training

All models are trained using the Adam optimizer with a learning rate of 0.0005, 10000 steps linear warm-up, $\beta = (0.9, 0.999)$, and batch size 64.

C Runtime

We perform runtime experiments using a single Nvidia GeForce GTX 1080 GPU and an Intel i7-8700@3.2GHz CPU. These experiments take into account all components of our traffic model, including input preparation, trajectory prediction, and action generation. The runtime results for all time step are recorded during the long-term evaluation, as shown in Fig. 4. We can see that the runtime increases almost linearly with the number of agents.

D Distribution

In Fig. 5, we illustrate the distribution of speed and distance to the leading vehicle during long-term simulations. Our method produces more similar speed distributions to the ground truth than SUMO since the Intelligent Driver Model (IDM) always aims to move at the highest speed. Furthermore, our method generates leader distance distributions that closely match the ground truth.

Figure 4: Runtime of each time step during the long-term evaluation.

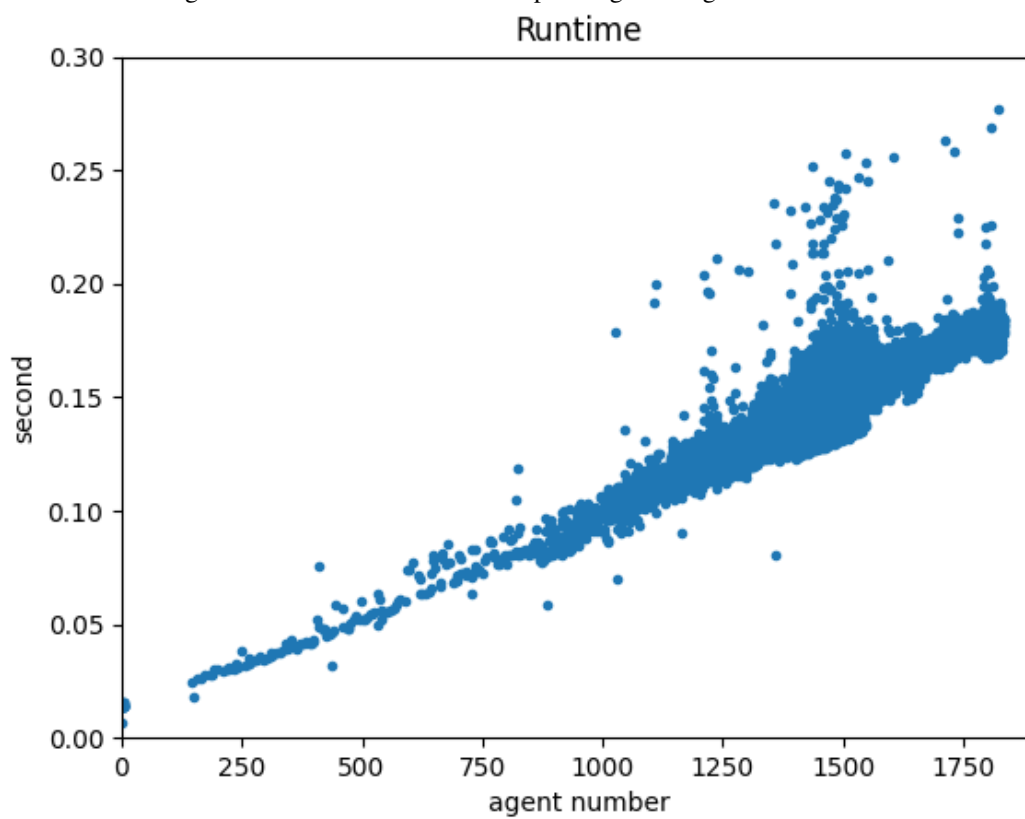


Figure 5: Distributions of speed and leader vehicle's distance in long-term evaluation.

